



Comparative studies for amyloid beta degradation: “Nepriylsin vs insulysin”, “monomeric vs aggregate”, and “whole A β_{40} vs its peptide fragments”

Dai Kato¹, Yoshiaki Takahashi², Haruto Iwata, Yusuke Hatakawa, Seon Hwa Lee, Tomoyuki Oe*

Department of Bio-analytical Chemistry, Graduate School of Pharmaceutical Sciences, Tohoku University, 6-3 Aramaki-aoba, Aoba-ku, Sendai, 980-8578, Japan

ARTICLE INFO

Keywords:
Amyloid beta
Nepriylsin
Insulysin
Insulin-degrading enzyme

ABSTRACT

Amyloid beta (A β) proteins are produced from amyloid precursor protein cleaved by β - and γ -secretases, and are the main components of senile plaques pathologically found in Alzheimer's disease (AD) patient brains. Therefore, the relationship between AD and A β s has been well studied for both therapeutic and diagnostic purposes. Several enzymes have been reported to degrade A β s *in vivo*, with nepriylsin (NEP) and insulysin (insulin-degrading enzyme, IDE) being the most prominent. In this article, we describe the mass spectrometric characterization of peptide fragments generated using NEP and IDE, and clarify the differences in digestion specificities between these two enzymes for non-aggregated A β_{40} , aggregated A β_{40} , and A β_{40} peptide fragments, including A β_{16} . Our results allowed identification of all the peptide fragments from non-aggregated A β_{40} : NEP, 23 peptide fragments consisting of 2–11 amino-acid residues, 17 cleavage sites; IDE, 23 peptide fragments consisting of 6–33 amino-acid residues, 15 cleavage sites. Also, we confirmed that IDE can digest only whole A β_{40} , whereas NEP can digest both A β_{40} and partial structures such as A β_{16} and peptide fragments generated by the digestion of A β_{40} by IDE. Furthermore, we confirmed that IDE and NEP are unable to digest aggregated A β_{40} .

1. Introduction

Alzheimer's disease (AD) is a progressive neurodegenerative disease that causes memory and cognitive impairment and accounts for about 50–56% of dementia cases worldwide [1,2]. The pathological features of AD include senile plaques and neurofibrillary tangles consisting of aggregated amyloid β (A β) proteins [1,2] and hyperphosphorylated tau proteins [3], respectively. Of these, the deposition of A β is recognized as the central event in the etiology of AD because it is the primary event in the disease process [4].

A β s are produced by cleavage of an integral membrane amyloid precursor protein (APP) at the N-terminus by β -secretase, followed by cleavage at the C-terminus by γ -secretase [5]. Variations in the position cleaved by γ -secretase generates several homologs with different lengths. A β_{40} and A β_{42} are the major homologs generated and are 40 and 42 amino-acid residues long, respectively. A β monomers can easily

aggregate under physiological conditions to form fibrils *via* soluble oligomers [6]. Neurotoxicity of the soluble oligomers [7] and synaptic plasticity/memory impairment caused by the dimer [8] have also been reported.

Almost twenty enzymes are known to contribute to A β degradation, including nepriylsin (NEP), insulysin (insulin-degrading enzyme, IDE), angiotensin-converting enzyme, and cathepsin B. The therapeutic utility of these enzymes in AD has been studied [9–12], including extensive studies of NEP and IDE in AD patients [13,14]. Furthermore, fluorescence assays for quantifying the enzyme activities of NEP and IDE have also been reported [15].

NEP is a zinc-dependent metalloprotease present in, for example, the brain, heart, peripheral vasculature, adrenal gland and lungs. NEP degrades not only A β but also a variety of bioactive peptides such as angiotensins and enkephalins [16]. In control mice, infusion of an NEP inhibitor (thiorphan) has been reported to induce A β_{40} and A β_{42} deposition and fibrillization [17], and in APP transgenic mice, the

* Corresponding author. Department of Bio-analytical Chemistry, Graduate School of Pharmaceutical Sciences, Tohoku University, Aoba-ku, Sendai, 980-8578, Japan.

E-mail address: t-oe@mail.pharm.tohoku.ac.jp (T. Oe).

¹ Dai KATO, Meiji Seika Pharma Co., Ltd., 4–16 Kyobashi 2-chome, Chuo-ku, Tokyo 104–8002, Japan.

² Yoshiaki TAKAHASHI, Technical Research Laboratory, Kyowa Hakko Bio Co., Ltd., 1-1 Kyowa-cho, Hofu-shi, Yamaguchi 747–8522, Japan.

Abbreviations

A β	amyloid beta
AD	Alzheimer's disease
APP	amyloid precursor protein
CSF	cerebrospinal fluid
EIC	extracted ion chromatogram
ESI	electrospray ionization
FA	formic acid
HFIP	1,1,1,3,3,3-hexafluoro-2-propanol
IDE	insulysin, insulin-degrading enzyme
LC	liquid chromatography
MeCN	acetonitrile

MS	mass spectrometry
MS/MS	tandem mass spectrometry
MS ⁿ	multiple-stage mass spectrometry
NEP	nepriylsin
ODS	octadecylsilyl
PBS	phosphate buffered saline;
PGC	porous graphitic carbon
r.t.	room temperature
THF	tetrahydrofuran
ThT	thioflavin T
TICC	total ion current chromatogram
t _R	retention time.

overexpression of NEP has been reported to reduce senile plaques [18].

IDE is also a zinc-dependent metalloprotease that is present in the liver, kidney, and brain [19] and degrades not only insulin and glucagon, but also A β s to regulate A β s *in vivo* [20]. In IDE-deficient mice, the degradation of A β was reduced by more than 50% concomitantly with the increase in the amount of A β in the brain [20], suggesting that IDE may be a link between AD and type 2 diabetes mellitus (which is a risk factor for AD) [21]. Therefore, A β -degrading enzymes such as NEP and IDE are recognized as key enzymes for AD therapy and as links between AD and its risk factors.

Generally, there are two major diagnostic strategies for AD: PET imaging using Pittsburgh Compound B (2-(4'-[¹¹C]methylaminophenyl)-6-hydroxybenzothiazole) for A β plaques and neurofibrillary tangles in brain [22], and the quantification of A β ₄₀, A β ₄₂, and tau in cerebrospinal fluid (CSF) using an immunosorbent assay or liquid chromatography (LC)-mass spectrometry (MS) [23]. However, there are few reported attempts to analyze specific A β peptide fragments generated by degrading enzymes, such as the *N*-terminal [24] and *C*-terminal [25] A β peptide fragments in CSF. Therefore, the potential use of specific A β peptide fragments generated by A β -degrading enzymes as clearance and diagnostic markers requires clarification of their detailed specificities, including details of the cleavage sites, the effect of combining several degrading enzymes, and the activities of the various components involved in the aggregation process (monomer, oligomer, and fibril).

In this article, we describe comparative studies on A β degradation conducted using two degrading enzymes (NEP vs. IDE), various sizes of A β (whole A β ₄₀ vs. its peptide fragments), and two aggregation states of A β (non-aggregated A β ₄₀ vs. aggregated A β ₄₀).

2. Materials and methods

2.1. Reagents and materials

Specific reagents and materials were purchased as follows: A β ₄₀ (human, DAEFRHDSGY EVHHQKLVFF AEDVGSNKGK IIGLMVGGVV) and A β ₁₆ (human, DAEFRHDSGY EVHHQK) (Anaspec, Inc., Fremont, CA, USA); NEP (human recombinant, solution in Tris, NaCl and ZnCl₂) (R&D Systems, Inc., Minneapolis, MN, USA); IDE (human recombinant, solution in Tris and NaCl) (Bon Opus Biosciences, LLC., Millburn, NJ, USA); sequencing grade modified trypsin (Promega Co., Madison, WI, USA); acetonitrile (MeCN), formic acid (FA), and tetrahydrofuran (THF) (Nacalai Tesque, Inc., Kyoto, Japan); thioflavin T (2-[4-(dimethylamino)phenyl]-3,6-dimethyl-1,3-benzothiazol-3-ium chloride, ThT) (Sigma-Aldrich, Inc., St. Louis, MO, USA); 1,1,1,3,3,3-hexafluoro-2-propanol

(HFIP) (Tokyo Chemical Industry Co., Ltd., Tokyo, Japan); OptiPlate-384, White Opaque 384-well MicroPlate (384 well plate) (PerkinElmer, Waltham, MA, USA); AMPLIseal (plate seal) (Greiner Bio-One, Baden-Württemberg, Germany); and Protein LoBind® tubes, 0.5 mL (Eppendorf, Hamburg, Germany). All other general chemicals, vials, and gases were of the highest grade available and were obtained from local providers.

2.2. Reagent solutions

All stock solutions were stored in Protein LoBind® tubes to minimize the adsorption of A β s.

Preparation and storage of A β ₄₀ (0.25 mM) solution: Lyophilized A β ₄₀ in its original vial was dissolved and monomerized in a corresponding amount of HFIP [26] to give a 1 mg/mL solution. This solution was sonicated for 8 min, incubated for 1 h, re-sonicated for 8 min at room temperature (r.t.), and evaporated to dryness under a N₂ stream. The residue was dissolved in a corresponding amount of 0.1% (v/v) aq. NH₄OH/MeCN (4:1, v/v) [27] to give a 0.25 mM solution. After 12 min sonication, the solution was divided into aliquots (30 μ L) and stored at -80 °C. Prior to use, the solutions were thawed, mixed by pipetting repeatedly (10 μ L, \times 10), then an aliquot was transferred into a tube (0.5 mL) and evaporated under a N₂ stream. The residue was re-dissolved in H₂O/MeCN (4:1, v/v) by sonicating for 3 min to give a 0.25 mM solution.

Preparation and storage of A β ₁₆ (0.55 mM) solution: Lyophilized A β ₁₆ in its original vial was dissolved in a corresponding amount of H₂O/MeCN (4:1, v/v) and sonicated for 12 min to give a 0.55 mM solution. The solution was divided into aliquots (30 μ L) and stored at -80 °C. Prior to use, the solution was thawed and used as-is.

Preparation and storage of ThT (0.125 mM) solution: ThT was dissolved in a corresponding amount of H₂O to give a 1.25 mM solution. The solution was divided into aliquots (50 μ L) and stored at -30 °C. Prior to use, the solution was thawed and diluted with PBS to give a 0.125 mM solution.

Preparation and storage of NEP solution: A commercially provided solution of NEP (0.44 μ g/ μ L, 22.7 μ L) was divided into aliquots (2.27 μ L) and stored as stock solutions at -30 °C. Prior to use, the solution was thawed and diluted with 25 mM Tris-HCl buffer (containing 200 mM NaCl and 5 μ M ZnCl₂) to give a 0.1 μ g/ μ L solution. This was further diluted with 10 mM PBS to give a 14 ng/ μ L solution.

Preparation and storage of IDE solution: A commercially provided solution of IDE (0.6 μ g/ μ L, 16.7 μ L) was diluted with 20 mM Tris-HCl buffer (containing 150 mM NaCl) to give a 0.1 μ g/ μ L solution. The

solution was divided into aliquots (10 μL) and stored as stock solutions at -80°C . Prior to use, the solution was thawed and diluted with 10 mM PBS to give a 14 ng/ μL solution.

Preparation and storage of trypsin solution: Lyophilized trypsin (20 μg) was dissolved in the supplied trypsin resuspension buffer (50 mM aq. acetic acid) to give a 0.1 $\mu\text{g}/\mu\text{L}$ solution. The solution was divided into aliquots (10 μL) and stored as stock solutions at -80°C . Prior to use, the solution was thawed and used as-is.

Control solution to monitor $\text{A}\beta_{40}$ aggregation: A mixture of $\text{A}\beta_{40}$ (0.25 mM, 10 μL), PBS (200 μL) and ThT (0.125 mM, 40 μL) was vortex-mixed for 30 s. The solution was mixed by repeated pipetting (75 $\mu\text{L} \times 5$), transferred to 3 wells (75 μL each) of a 384 well plate, and covered with a plate seal for use in ThT assays [28]. The blank sample was prepared with $\text{H}_2\text{O}/\text{MeCN}$ (4:1, v/v, 10 μL) instead of $\text{A}\beta_{40}$ (0.25 mM, 10 μL) and transferred to 3 wells (75 μL each).

2.3. Proteolysis of $\text{A}\beta_{40}$ or $\text{A}\beta_{16}$

All the reactions were performed in Protein LoBind® tubes except for the ThT assay. Digestion studies were performed using a ratio of $\text{A}\beta$ (substrate):enzyme = 40:1 (w/w).

Digestion of non-aggregated $\text{A}\beta_{40}$ by NEP or IDE: A mixture of $\text{A}\beta_{40}$ (0.25 mM, 15 μL), PBS (105 μL), and NEP or IDE (14 ng/ μL , 30 μL) was incubated at 37°C for 1, 3, and 7 days.

Digestion of non-aggregated $\text{A}\beta_{40}$ by both NEP and IDE: A mixture of $\text{A}\beta_{40}$ (0.25 mM, 15 μL), PBS (105 μL), NEP (14 ng/ μL , 15 μL) and IDE (14 ng/ μL , 15 μL) was incubated at 37°C for 3 and 7 days.

Digestion of non-aggregated $\text{A}\beta_{40}$ by IDE followed by NEP: A mixture of $\text{A}\beta_{40}$ (0.25 mM, 30 μL), PBS (210 μL) and IDE (14 ng/ μL , 60 μL) was incubated at 37°C for 7 days. An aliquot of the solution (100 μL) and NEP (14 ng/ μL , 20 μL) was mixed and incubated at 37°C for 7 days. As a control, an aliquot of the solution (100 μL) and PBS (20 μL) was incubated at 37°C for 3 days.

Digestion of $\text{A}\beta_{16}$ by NEP or IDE: A mixture of $\text{A}\beta_{16}$ (0.55 mM, 10 μL), PBS (70 μL), and NEP or IDE (14 ng/ μL , 20 μL) was incubated at 37°C for 3 days.

Digestion of aggregated $\text{A}\beta_{40}$ by IDE, NEP, or trypsin: A mixture of $\text{A}\beta_{40}$ (0.25 mM, 20 μL) and PBS (480 μL) was vortex-mixed for 30 s. The solution was mixed by repeated pipetting (75 $\mu\text{L} \times 5$), transferred to wells (75 μL each) of a 384 well plate, and covered with a plate seal. After incubation at 37°C for 24 h in a Gemini XPS microplate spectrofluorometer (Molecular Devices, LLC, San Jose, CA, USA), IDE, NEP, or trypsin (0.1 $\mu\text{g}/\mu\text{L}$, 0.81 μL) was added and the mixture was incubated at 37°C for 3 and 7 days. Aggregation was confirmed by the ThT assay using the above control solution to monitor $\text{A}\beta_{40}$ aggregation.

2.4. Conditions for the ThT assay

A Gemini XPS microplate spectrofluorometer was used in kinetic mode with the following parameters: temperature, 37°C ; read mode, top read; wavelength, ex. 456, em. 489 nm; sensitivity, 12 readings PMT sensitivity Medium; run time, 24 h; interval, 15 min; automix, before first read, 15 s; between reads, 300 s; autocalibrate, on; assay plate type, 384 well standard clrbtm; column priority; carriage speed, normal; and auto read, off. SoftMax Pro Software (version 5.4.1, Molecular Devices) was used for data analysis. The data were organized using Microsoft Excel 2016 (Microsoft Corporation, Redmond, WA, USA) to calculate the average, relative error. The fluorescence intensities were used after subtracting the corresponding controls.

2.5. LC conditions

An Agilent 1100 HPLC system (Agilent Technologies, Inc., Santa

Clara, CA, USA) equipped with a 1100 G1312A binary pump, 1100 G1379A degasser, 1100 G1367A autosampler, 1100 G1316A column heater, and a 1100 G1315B photodiode array was used for LC systems 1–4 with the following common chromatographic conditions: Mobile phases (A) 0.1% (v/v) FA in H_2O , (B) 0.1% (v/v) FA in MeCN; flow rate 0.2 mL/min; and column temperature, 40°C .

LC system 1 (for hydrophobic peptide fragments from non-aggregated $\text{A}\beta_{40}$): A Cosmosil® 5C₁₈-AR-II (octadecylsilyl, ODS) column (150 \times 2.0 mm i.d., 5 μm , 120 \AA ; Nacalai Tesque, Inc.) was used with the following linear gradient: 0 min, 0% B; 140 min, 42% B; 141 min, 65% B; 155 min, 65% B; 156 min, 20% B; 165 min, 45% B; 166 min, 20% B; 175 min, 45% B; 176 min, 20% B; 185 min, 45% B; 186 min, 20% B; 195 min, 45% B; 196 min, 20% B; 205 min, 45% B; 206 min, 20% B; 215 min, 45% B; 216 min, 0% B; and 240 min, 0% B. An aliquot of the solution (20 μL) was injected into the system. The eluate obtained between 3–140 min was introduced into the MS system.

LC system 2 (for polar peptide fragments from non-aggregated $\text{A}\beta_{40}$ and $\text{A}\beta_{16}$): A Hypercarb™ porous graphitic carbon (PGC) column [29] (100 \times 2.1 mm i.d., 5 μm ; Thermo Fischer Scientific Inc., Waltham, MA, USA) was used with the following linear gradient: 0 min, 0% B; 100 min, 50% B; 101 min, 65% B; 115 min, 65% B; 116 min, 0% B; and 140 min, 0% B. An aliquot of the solution (20 μL) was injected into the system. The eluate obtained between 3–100 min was introduced into the MS system.

LC system 3 (for hydrophobic peptide fragments from $\text{A}\beta_{16}$): A Cosmosil® 5C₁₈-AR-II column (150 \times 2.0 mm i.d., 5 μm , 120 \AA ; Nacalai Tesque, Inc.) was used with the following linear gradient: 0 min, 0% B; 140 min, 42% B; 141 min, 65% B; 155 min, 65% B; 156 min, 0% B; and 180 min, 0% B. An aliquot of the solution (15 μL) was injected into the system. The eluate obtained between 3–140 min was introduced into the MS system.

LC system 4 (for hydrophobic peptide fragments from aggregated $\text{A}\beta_{40}$): A Cosmosil® 5C₁₈-AR-II column (150 \times 2.0 mm i.d., 5 μm , 120 \AA ; Nacalai Tesque, Inc.) was used with the following linear gradient: 0 min, 0% B; 140 min, 42% B; 141 min, 65% B; 155 min, 65% B; 156 min, 20% B; 165 min, 45% B; 166 min, 20% B; 175 min, 45% B; 176 min, 20% B; 185 min, 45% B; 186 min, 20% B; 195 min, 45% B; 196 min, 20% B; 205 min, 45% B; 206 min, 20% B; 215 min, 45% B; 216 min, 0% B; and 240 min, 0% B. THF (50 μL) was injected tenth at 4-min intervals from 160 min to prevent carryover. An aliquot of the solution (30 μL) was injected into the system. The eluate obtained between 3–140 min was introduced into the MS system.

2.6. MS conditions

An LCQ-DECA ion-trap mass spectrometer (Thermo Fischer Scientific Inc.) equipped with an electrospray ionization (ESI) source was used in positive ion mode with the following parameters: spray voltage, 4.5 kV; capillary temperature, 300°C ; sheath gas flow rate, 85.0 arb; and auxiliary gas flow rate, 15.0 arb. The parameters for data-dependent MS/MS were as follows: Full scan range, m/z 100–2000 (for LC systems 1, 3, and 4) or 100–1000 (for LC system 2); precursor, top 3 ions; default charge state, 2; default isolation width, 2; normalized collision energy (CE), 45%; activation Q, 0.25; activation time, 30 ms; minimum MS signal required, 100,000; and minimum MSⁿ signal required, 5000. Xcalibur™ (version 2.0 SR2) was used for the data analyses.

2.7. Criteria for identification of peptide fragments

Proteome Discoverer (version 1.3) (Thermo Fischer Scientific Inc.) was used to identify peptide fragments using the following parameters: Minimum precursor mass, 100 Da; maximum precursor mass, 5000 Da; enzyme, no-enzyme (unspecific); precursor mass tolerance, 2 Da;

fragment mass tolerance, 0.8 Da; dynamic modification, oxidation (methionine); target false discovery rate (strict), 0.01; and target false discovery rate (relaxed), 0.05. All the identified peptide fragments were confirmed by checking the MS/MS spectra.

3. Results and discussion

3.1. General experimental setting

A β s are challenging proteins to handle and analyze because they tend to adsorb and aggregate, and their concentration often changes because they adsorb on tubes and proteins [30]. Furthermore, significant carryover from previous injections occurs during HPLC analyses [31]. Therefore, A β ₄₀ was initially monomerized using HFIP [26] and stored as a 0.1% (v/v) aq. NH₄OH/MeCN (4:1, v/v) solution [27]. The ODS column was washed using a quick zigzag gradient alternating between 20% B and 45% B before column equilibration (LC systems 1 and 4). Multiple injections of THF were made for LC system 4 (for aggregated A β ₄₀). Short peptides are generally too polar (hydrophilic) to be retained on versatile ODS columns. Therefore, we concomitantly used a PGC column, which is good for hydrophilic peptides [29], to cover all the peptide fragments.

3.2. Non-aggregated A β ₄₀ incubated with NEP

A β ₄₀ was digested into 23 peptide fragments (2–11 amino-acid residues, 17 cleavage sites) (Fig. 1) without residual intact A β ₄₀ after 3 days. Interestingly, the intensity patterns of several peptide peaks changed during prolonged incubation up to 7 days (Fig. 1): the peak corresponding to F²⁰AEDVGSNKGA³⁰ (m/z 1094.43, retention time (t_R) = 28.30 min on ODS) decreased as the intensities of the peaks corresponding to F²⁰AEDVGSNK²⁸ (m/z 966.33, t_R = 25.74 min on ODS) and F²⁰AEDVG²⁵ (m/z 637.12, t_R = 33.65 min on ODS) increased, suggesting that long peptide fragments can be further digested by NEP. Each amino acid sequence and its t_R identified by LC-MS with LC systems 1 and 2 is summarized in Table 1.

3.3. Non-aggregated A β ₄₀ incubated with IDE

A β ₄₀ was digested into 23 peptide fragments. The intensity of each peak gradually increased in a time-dependent manner on the decrease in residual A β ₄₀. However, some A β ₄₀ remained even after 7 days, suggesting that IDE is less active than NEP in degrading A β ₄₀ in our experimental setting (Fig. 2). The peptide fragments tended to be longer (5–33 amino-acid residues, 15 cleavage sites), and most of the peptide fragments were longer than 12 amino-acid residues, except for G²⁹AIIG³³, M³⁵VGGVV⁴⁰, and L³⁴MVGGVV⁴⁰. In contrast, the longest peptide fragment obtained using NEP consisted of 11 amino-acid residues. Each amino acid sequence and its t_R identified by LC-MS with LC systems 1 and 2 is summarized in Table 2.

3.4. Non-aggregated A β ₄₀ incubated with both NEP and IDE

Since multiple proteases are involved in A β elimination *in vivo*, A β ₄₀ was incubated with both NEP and IDE (Fig. 3). The total ion current chromatogram (TICC) and the identified peptide fragments were almost identical to those obtained using NEP only (Fig. 1). In addition, the long peptide fragments listed in Table 2 (12~ amino-acid residues, obtained using IDE) were not detected, suggesting that the long fragment peptide generated by IDE was further digested by NEP. Each amino acid sequence and its t_R identified by LC-MS with LC systems 1 and 2 is summarized in Table 3.

3.5. Non-aggregated A β ₄₀ incubated with IDE followed by NEP

Since the experiment above suggested that the long fragment peptide obtained using IDE could be further digested by NEP, A β ₄₀ was incubated with IDE, followed by digestion using NEP. The TICC pattern of the peptide fragments (Fig. 4) was identical to the one obtained using NEP only (Fig. 1). In addition, the long peptide fragments obtained by digestion with IDE (12~ amino acid residues) were not detected, similar to the results obtained by digestion with both NEP and IDE (Fig. 3), confirming that the long fragment peptides obtained using IDE were

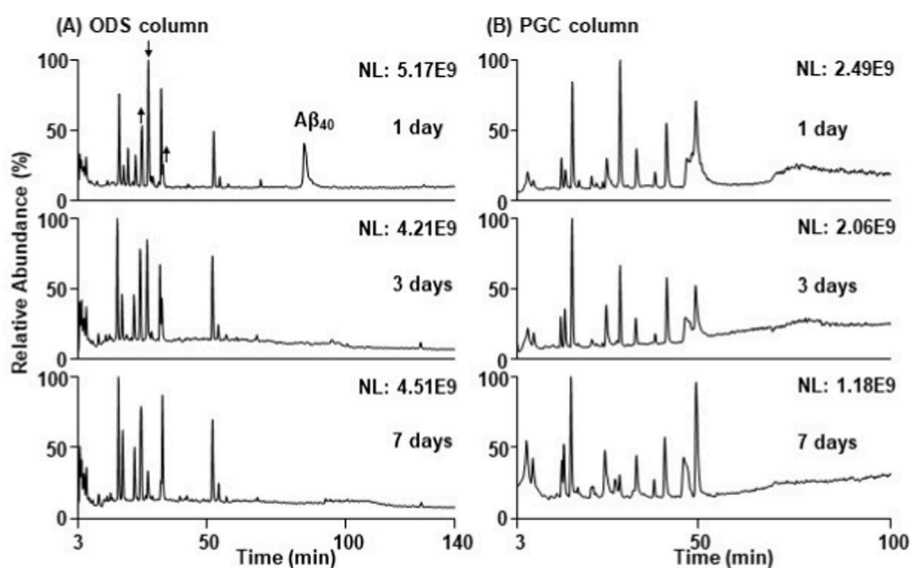


Fig. 1. TICCs of non-aggregated A β ₄₀ incubated with NEP for 1 day (top), 3 days (middle), and 7 days (bottom). (A) LC system 1 (ODS for hydrophobic peptides), (B) LC system 2 (PGC for polar peptides). Identified peptides are shown in Table 1, together with the charge state, precursor MS (m/z), and t_R (min). Arrows in the chromatogram (ODS/1 day) indicate that the amount of the peptide increased (↑) or decreased (↓) during prolonged incubation.

Table 1
Peptide fragments found from non-aggregated A β ₄₀ incubated with NEP.

Sequence number	Sequence	Charge	<i>m/z</i>	<i>t_R</i> (min)	LC	
12 - 17	VHHQKL	1	761.37	3.70	ODS	
4 - 9	FRHDSG	1	718.33	4.29		
10 - 11	YE	1	311.02	5.21		
39 - 40	VV	1	216.95	6.03		
21 - 29	AEDVGSNKG	1	876.27	10.44		
31 - 33	IIG	1	301.97	17.54		
20 - 22	FAE	1	365.93	18.68		
34 - 35	LM	1	262.99	19.13		
10 - 17	YEVHHQKL	4	264.98	23.45		
20 - 28	FAEDVGSNK	1	966.33	25.74		
20 - 29	FAEDVGSNKG	1	1023.39	25.85		
20 - 30	FAEDVGSNKG	1	1094.43	28.30		
34 - 38	LMVGG	1	476.03	33.08		
20 - 25	FAEDVG	1	637.12	33.65		
17 - 19	LVF	1	378.00	51.90		
31 - 34	IIGL	1	415.07	54.11		
34 - 40	LMVGGVV	1	674.24	68.28		
39 - 40	VV	1	217.00	5.44		PGC
36 - 38	VGG	1	232.00	7.06		
1 - 3	DAE	1	333.99	14.59		
34 - 35	LM	1	263.02	15.19		
31 - 33	IIG	1	301.99	16.95		
23 - 28	DVGSNK	1	619.51	19.55		
23 - 29	DVGSNKG	1	676.31	22.47		
18 - 19	VF	1	265.08	25.83		
21 - 29	AEDVGSNKG	1	876.35	28.38		
34 - 38	LMVGG	1	476.11	29.56		
4 - 5	FR	1	322.18	33.15		
10 - 11	YE	1	311.07	33.94		
20 - 22	FAE	1	365.97	38.29		
31 - 34	IIGL	1	415.13	38.53		
17 - 19	LVF	1	378.02	41.31		
20 - 28	FAEDVGSNK	1	966.37	46.25		
20 - 25	FAEDVG	1	637.10	49.44		

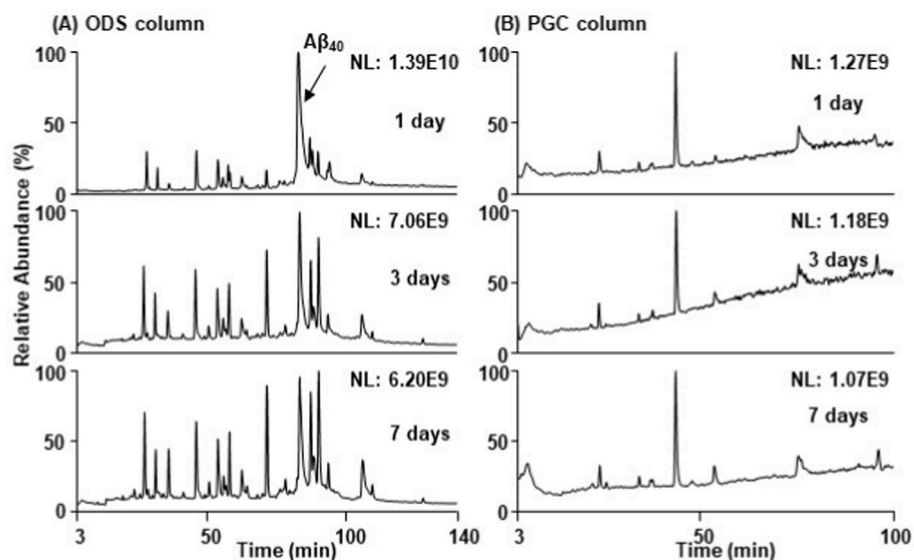


Fig. 2. TICs of non-aggregated A β ₄₀ incubated with IDE for 1 day (top), 3 days (middle), and 7 days (bottom). (A) LC system 1 (ODS for hydrophobic peptides), (B) LC system 2 (PGC for polar peptides). Identified peptides are shown in Table 2, together with the charge state, precursor MS (*m/z*), and *t_R* (min).

Table 2
Peptide fragments found from non-aggregated A β ₄₀ incubated with IDE.

Sequence number	Sequence	Charge	<i>m/z</i>	<i>t_R</i> (min)	LC	
2 - 14	AEFRHDSGYEVHH	2	792.32	23.57	ODS	
1 - 14	DAEFRHDSGYEVHH	2	850.04	27.25		
1 - 13	DAEFRHDSGYEVH	2	781.36	31.27		
1 - 18	DAEFRHDSGYEVHHQKLV	3	723.21	35.99		
35 - 40	MVGGVV	1	561.01	41.26		
1 - 19	DAEFRHDSGYEVHHQKLVF	3	772.38	45.92		
14 - 28	HQKLVFFAEDVGSNK	2	860.15	50.69		
1 - 28	DAEFRHDSGYEVHHQKLVFFAEDVGSNK	3	1088.09	53.85		
1 - 20	DAEFRHDSGYEVHHQKLVFF	3	821.44	55.83		
16 - 28	KLVFFAEDVGSNK	2	727.43	56.64		
34 - 40	LMVGGVV	1	674.19	58.04		
1 - 33	DAEFRHDSGYEVHHQKLVFFAEDVGSNKGAIIG	3	1225.24	62.50		
17 - 28	LVFFAEDVGSNK	1	1325.35	64.37		
17 - 31	LVFFAEDVGSNKGAI	2	783.29	71.49		
28 - 40	KGAIIGLMVGGVV	2	607.36	77.43		
27 - 40	NKGAIIGLMVGGVV	2	664.45	78.14		
21 - 40	AEDVGSNKGAIIGLMVGGVV	2	943.40	83.34		
20 - 40	FAEDVGSNKGAIIGLMVGGVV	2	1017.42	87.25		
14 - 40	HQKLVFFAEDVGSNKGAIIGLMVGGVV	3	929.37	88.29		
29 - 40	GAIIGLMVGGVV	1	1085.38	90.13		
19 - 40	FFAEDVGSNKGAIIGLMVGGVV	2	1090.75	93.61		
8 - 31	SGYEVHHQKLVFFAEDVGSNKGAI	2	1316.89	106.11		
29 - 33	GAIIG	1	430.00	24.24		PGC
35 - 40	MVGGVV	1	561.09	34.41		
34 - 40	LMVGGVV	1	674.19	43.83		

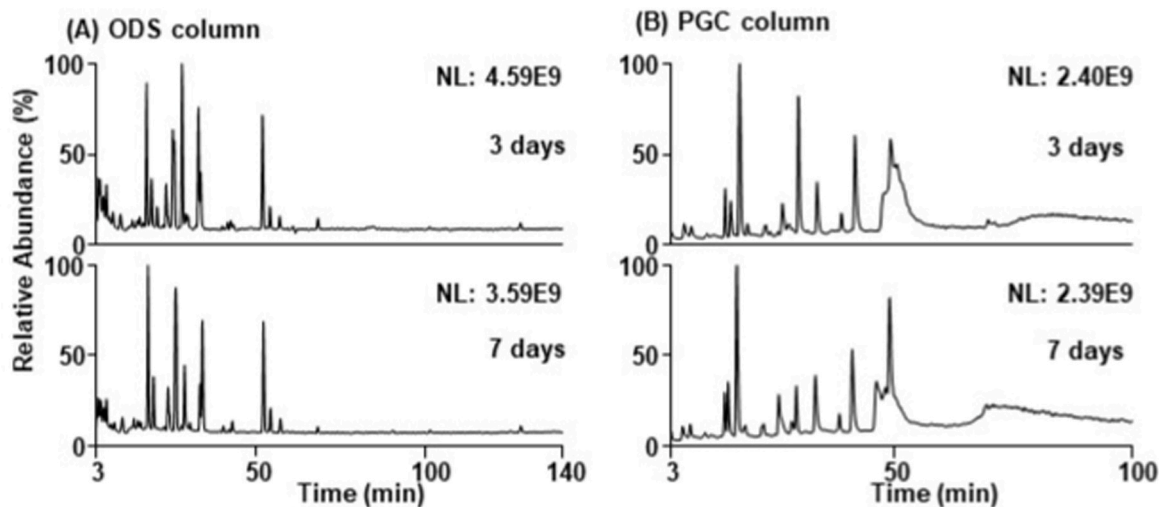


Fig. 3. TICCs of non-aggregated A β ₄₀ incubated with both NEP and IDE for 3 days (top) and 7 days (bottom). (A) LC system 1 (ODS for hydrophobic peptides), (B) LC system 2 (PGC for polar peptides). Identified peptides are shown in Table 3, together with the charge state, precursor MS (*m/z*), and *t_R* (min).

further digested by NEP. Each amino acid sequence and its *t_R* identified by LC-MS with LC system 1 is summarized in Table 4.

3.6. A β ₁₆ incubated with NEP or IDE

To further compare the digestion patterns between NEP and IDE, a shorter A β ₄₀ homologue (A β ₁₆) was incubated with IDE or NEP. The amino acid sequence of A β ₁₆ contains 4 and 5 cleavage sites identified in experiments using A β ₄₀ digested by NEP (Table 1) and IDE (Table 2), respectively. The cleavage sites, shown as slashes, are: NEP, DAE/FR/HDSG/YE/VHHQK; IDE, D/AEFRHD/SGYEVH/H/Q/K. Thus, A β ₁₆ was

digested by NEP into the five peptides D¹AE³, F⁴R⁵, H⁶DSG⁹, Y¹⁰E¹¹, and V¹²HHQK¹⁶ (Fig. 5 AB), and the cleavage sites were identical to those in A β ₄₀. In contrast, A β ₁₆ was not digested by IDE (Fig. 5CD). These results suggest that IDE digests A β ₄₀ by recognizing the whole structure, whereas NEP digests A β ₄₀ by recognizing the partial structure.

3.7. Aggregated A β ₄₀ incubated with NEP, IDE or trypsin

The A β sequence has an amphipathic character because the *N*-terminal segment is hydrophilic whereas the *C*-terminal segment is hydrophobic. Monomeric A β prefers to adopt random coil or α -helix

Table 3
Peptide fragments found from non-aggregated A β ₄₀ incubated with both NEP and IDE.

Sequence number	Sequence	Charge	<i>m/z</i>	<i>t_R</i> (min)	LC
12 - 17	VHHQKL	1	761.02	3.69	ODS
4 - 9	FRHDSG	1	718.00	4.28	
10 - 11	YE	1	310.75	5.18	
39 - 40	VV	1	216.67	6.04	
21 - 28	AEDVGSNK	2	410.02	8.35	
21 - 29	AEDVGSNKG	2	438.53	10.79	
35 - 38	MVGG	1	362.69	14.15	
31 - 33	IIG	1	301.66	18.28	
20 - 22	FAE	1	365.69	19.53	
34 - 35	LM	1	262.69	19.80	
10 - 17	YEVHHQKL	4	264.66	24.17	
20 - 28	FAEDVGSNK	2	483.66	26.36	
20 - 29	FAEDVGSNKG	2	512.20	26.55	
20 - 30	FAEDVGSNKGGA	2	547.70	29.00	
34 - 38	LMVGG	1	475.71	33.50	
20 - 25	FAEDVG	1	636.78	34.26	
17 - 19	LVF	1	377.68	52.14	
31 - 34	IIGL	1	414.70	54.25	
18 - 20	VFF	1	411.71	57.15	
34 - 40	LMVGGVV	1	673.89	68.11	
39 - 40	VV	1	216.74	5.52	PGC
36 - 38	VGG	1	231.68	7.10	
1 - 3	DAE	1	333.68	14.30	
34 - 35	LM	1	262.76	15.03	
31 - 33	IIG	1	301.73	16.85	
35 - 38	MVGG	1	362.71	18.54	
21 - 25	AEDVG	1	489.71	22.40	
18 - 19	VF	1	264.75	25.59	
21 - 29	AEDVGSNKG	2	438.47	28.27	
34 - 38	LMVGG	1	475.77	29.29	
10 - 11	YE	1	310.74	33.29	
20 - 22	FAE	1	365.68	37.74	
31 - 34	IIGL	1	414.76	38.35	
17 - 19	LVF	1	377.02	41.01	
20 - 28	FAEDVGSNK	2	483.69	46.67	
20 - 29	FAEDVGSNKG	2	512.01	48.02	
20 - 25	FAEDVG	1	636.85	48.93	

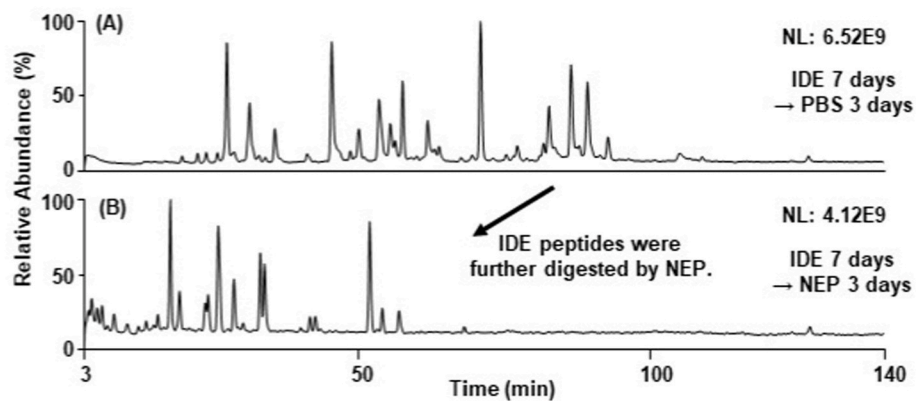


Fig. 4. TICCs of non-aggregated A β ₄₀ incubated with IDE, followed by NEP. (A) Control (incubated with IDE only), (B) experiment (incubated with IDE, followed by NEP). Identified peptides are shown in Table 4, together with the charge state, precursor MS (*m/z*), and *t_R* (min).

Table 4
Peptide fragments found from non-aggregated A β ₄₀ incubated with IDE followed by NEP.

Sequence number	Sequence	Charge	<i>m/z</i>	<i>t_R</i> (min)	LC
12 - 17	VHHQKL	1	761.13	3.62	ODS
4 - 9	FRHDSG	1	718.18	4.31	
10 - 11	YE	1	310.84	5.22	
39 - 40	VV	1	216.81	6.04	
21 - 28	AEDVGSNK	1	819.11	8.08	
21 - 29	AEDVGSNKG	2	438.50	10.35	
35 - 38	MVGG	1	362.82	13.55	
31 - 33	IIG	1	301.79	17.76	
20 - 22	FAE	1	365.86	18.96	
34 - 35	LM	1	262.79	19.32	
10 - 17	YEVHHQKL	4	264.83	23.62	
20 - 28	FAEDVGSNK	2	483.66	25.99	
20 - 29	FAEDVGSNKG	2	512.27	26.30	
20 - 30	FAEDVGSNKGA	2	547.76	28.67	
34 - 38	LMVGG	1	475.90	33.15	
20 - 25	FAEDVG	1	636.94	33.90	
19 - 28	FFAEDVGSNK	2	557.35	41.71	
14 - 18	HQKLV	2	312.84	42.63	
17 - 19	LVF	1	377.84	51.95	
31 - 34	IIGL	1	414.90	54.09	
18 - 20	VFF	1	411.84	57.00	
34 - 40	LMVGGVV	1	674.01	68.18	

structures, but gradually changes to a β -sheet structure during the aggregation process [6]. Aggregated A β ₄₀ was prepared by monitoring using the ThT assay, which is a β -sheet-specific fluorescence assay used as the “gold standard” for selectively identifying amyloid fibrils [28]. The fluorescence intensity was maximum after 24 h incubation and then remained essentially unchanged. After confirming aggregation, a control solution prepared without ThT (no ThT in the digestion samples) was mixed with NEP, IDE, or trypsin (positive control, cleavage at the C-terminus of R and K), and incubated at 37 °C. Aggregated A β ₄₀ was not digested by either NEP or IDE by prolonged incubation up to 7 days (Fig. 6AB), suggesting that A β ₄₀ gained resistance against digestion by both NEP and IDE. In contrast, aggregated A β ₄₀ was digested by trypsin to form four peptide fragments: D¹AEFR⁵, H⁶DSGYEVHHQK¹⁶, L¹⁷VFFAEDVGSNK²⁸, and G²⁹AIIGLMVGGVV⁴⁰ (Fig. 6C).

4. Conclusion

In this article, we described the mass spectrometric characterization of the digestion specificities of NEP and IDE for non-aggregated A β ₄₀, aggregated A β ₄₀, and A β ₄₀ peptide fragments, including A β ₁₆. Howell et al. [32] and Leissring et al. [33] reported similar degradation studies but overlooked several polar peptide fragments and did not examine the relationship between NEP and IDE. We identified all the peptide fragments from non-aggregated A β ₄₀, as follows (Fig. 7): NEP, 23 peptide fragments consisting of 2–11 amino-acid residues (17 cleavage sites), and for IDE, 23 peptide fragments consisting of 6–33 amino-acid residues (15 cleavage sites). Our use of a PGC column [29] made it possible to retain polar peptide fragments and to identify novel cleavage sites: for example, a recent review suggested that A β ₄₀ is cleaved at only 10 and 5 sites by NEP and IDE, respectively [12]. Also, we confirmed that IDE can digest only whole A β ₄₀, in contrast with NEP, which can digest whole A β ₄₀, partial structures such as A β ₁₆, and peptide fragments generated

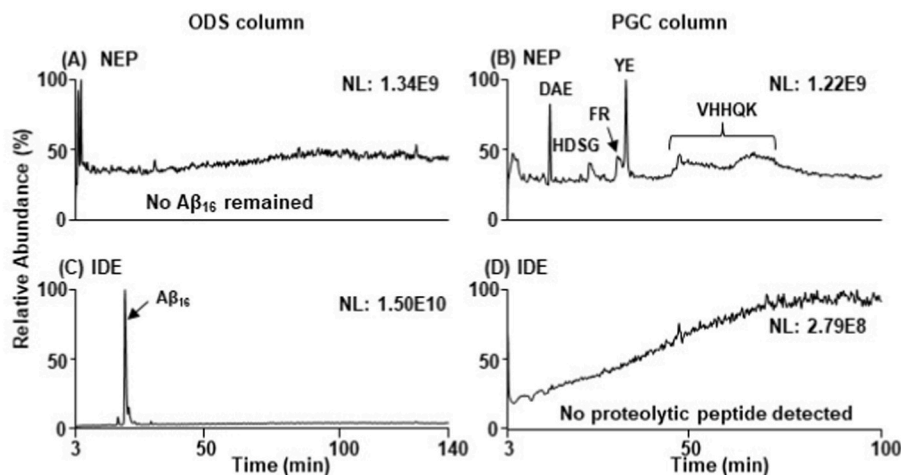


Fig. 5. TICCs of non-aggregated A β ₁₆ incubated with NEP (A and B) or IDE (C and D). LC system 3 (ODS for hydrophobic peptides) was used for (A) and (C). LC system 2 (PGC for polar peptides) was used for B and D.

CRediT author contribution statement

Dai KATO: Investigation, Data Curation, Visualization. Yoshiaki TAKAHASHI: Investigation, Data Curation. Haruto IWATA: Investigation, Data Curation. Yusuke HATAKAWA: Project administration. Seon Hwa LEE: Project administration, Writing - Review & Editing. Tomoyuki OE: Supervision, Conceptualization, Methodology, Writing - Original Draft, Writing - Review & Editing, Funding acquisition.

Declaration of competing interest

The authors declare that there is no conflict of interest.

Data availability

Data will be made available on request.

Acknowledgements

This work was supported in part by Grants-in-Aid for Challenging Exploratory Research (to T.O., # 21659035 for 2009–2011) and Scientific Research (B) (to T.O., # 16H05078 for 2016–2018) from the Japan Society for the Promotion of Science (JSPS). The authors thank Astellas Pharma Inc. (Tsukuba, Japan) for donating a used LCQ DECA.

References

- H.W. Querfurth, F.M. LaFerla, Alzheimer's disease, *N. Engl. J. Med.* 362 (2010) 329–344, <https://doi.org/10.1056/NEJMra0909142>.
- D.J. Selkoe, Alzheimer's disease: genes, proteins, and therapy, *Phys. Rev.* 81 (2001) 741–766, <https://doi.org/10.1152/physrev.2001.81.2.741>.
- V.M.-Y. Lee, M. Goedert, J.Q. Trojanowski, Neurodegenerative tauopathies, *Annu. Rev. Neurosci.* 24 (2001) 1121–1159, <https://doi.org/10.1146/annurev.neuro.24.1.1121>.
- J. Hardy, D. Allsop, Amyloid deposition as the central event in the aetiology of Alzheimer's disease, *Trends Pharmacol. Sci.* 12 (1991) 383–388, [https://doi.org/10.1016/0165-6147\(91\)90609-V](https://doi.org/10.1016/0165-6147(91)90609-V).
- H.M. Wilkins, R.H. Swerdlow, Amyloid precursor protein processing and bioenergetics, *Brain Res. Bull.* 133 (2017) 71–79, <https://doi.org/10.1016/j.brainresbull.2016.08.009>.
- V.H. Finder, R. Glockshuber, Amyloid-beta aggregation, *Neurodegener. Dis.* 4 (2007) 13–27, <https://doi.org/10.1159/000100355>.
- R. Kaye, E. Head, J.L. Thompson, T.M. McIntire, S.C. Milton, C.W. Cotman, C. G. Glabe, Common structure of soluble amyloid oligomers implies common mechanism of pathogenesis, *Science* 300 (2003) 486–489, <https://doi.org/10.1126/science.1079469>.
- G.M. Shankar, S. Li, T.H. Mehta, A. Garcia-Munoz, N.E. Shepardson, I. Smith, F. M. Brett, M.A. Farrell, M.J. Rowan, C.A. Lemere, C.M. Regan, D.M. Walsh, B. L. Sabatini, D.J. Selkoe, Amyloid-beta protein dimers isolated directly from Alzheimer's brains impair synaptic plasticity and memory, *Nat. Med.* 14 (2008) 837–842, <https://doi.org/10.1038/nm1782>.
- N.N. Nalivaeva, C. Beckett, N.D. Belyaev, A.J. Turner, Are amyloid-degrading enzymes viable therapeutic targets in Alzheimer's disease? *J. Neurochem.* 120 (2012) 167–185, <https://doi.org/10.1111/j.1471-4159.2011.07510.x>.
- L. Morelli, R. Llovera, S. Ibendahl, E.M. Castaño, The degradation of amyloid β as a therapeutic strategy in Alzheimer's disease and cerebrovascular amyloidoses, *Neurochem. Res.* 27 (2002) 1387–1399, <https://doi.org/10.1023/A:1021679817756>.
- J.S. Miners, N. Barua, P.G. Kehoe, S. Gill, S. Love, A β -degrading enzymes: potential for treatment of Alzheimer disease, *J. Neuropathol. Exp. Neurol.* 70 (2011) 944–959, <https://doi.org/10.1097/NEN.0b013e3182345e46>.
- N.L. Sikanyika, H.C. Parkinson, A.I. Smith, S. Kuruppu, Powering amyloid beta degrading enzymes: a possible therapy for Alzheimer's disease, *Neurochem. Res.* 44 (2019) 1289–1296, <https://doi.org/10.1007/s11064-019-02756-x>.
- S. Vepsäläinen, S. Helisalmi, A. Mannermaa, T. Pirttilä, H. Soininen, M. Hiltunen, Combined risk effects of IDE and NEP gene variants on Alzheimer disease, *J. Neurol. Neurosurg. Psychiatry* 80 (2009) 1268–1270, <https://doi.org/10.1136/jnnp.2008.160002>.
- J.S. Miners, S. Baig, H. Tayler, P.G. Kehoe, S. Love, Neprilysin and insulin-degrading enzyme levels are increased in Alzheimer disease in relation to disease severity, *J. Neuropathol. Exp. Neurol.* 68 (2009) 902–914, <https://doi.org/10.1097/NEN.0b013e3181afe475>.
- P.-T. Chen, T.-Y. Liao, C.-J. Hu, S.-T. Wu, S.S.-S. Wang, R.P.-Y. Chen, A highly sensitive peptide substrate for detecting two A β -degrading enzymes: neprilysin and insulin-degrading enzyme, *J. Neurosci. Methods* 190 (2010) 57–62, <https://doi.org/10.1016/j.jneumeth.2010.04.024>.
- A. Bayes-Genis, J. Barallat, A.M. Richards, A test in context: neprilysin: function, inhibition, and biomarker, *J. Am. Coll. Cardiol.* 68 (2016) 639–653, <https://doi.org/10.1016/j.jacc.2016.04.060>.
- I. Dolev, D.M. Michaelson, A nontransgenic mouse model shows inducible amyloid- β (A β) peptide deposition and elucidates the role of apolipoprotein E in the amyloid cascade, *Proc. Natl. Acad. Sci. U.S.A.* 101 (2004) 13909–13914, <https://doi.org/10.1073/pnas.0404458101>.
- R.A. Marr, E. Rockenstein, A. Mukherjee, M.S. Kindy, L.B. Hersh, F.H. Gage, I. M. Verma, E. Masliah, Neprilysin gene transfer reduces human amyloid pathology in transgenic mice, *J. Neurosci.* 23 (2003) 1992–1996, <https://doi.org/10.1523/JNEUROSCI.23-06-01992.2003>.
- R.E. Hulse, L.A. Ralat, T. Wei-Jen, Structure, function, and regulation of insulin-degrading enzyme, *Vitam. Horm.* 80 (2009) 635–648, [https://doi.org/10.1016/S0083-6729\(08\)00622-5](https://doi.org/10.1016/S0083-6729(08)00622-5).
- W. Farris, S. Mansourian, Y. Chang, L. Lindsley, E.A. Eckman, M.P. Froesch, C. B. Eckman, R.E. Tanzi, D.J. Selkoe, S. Guénette, Insulin-degrading enzyme regulates the levels of insulin, amyloid β -protein, and the β -amyloid precursor protein intracellular domain *in vivo*, *Proc. Natl. Acad. Sci. U.S.A.* 100 (2003) 4162–4167, <https://doi.org/10.1073/pnas.0230450100>.
- E.M.C. Schrijvers, J.C.M. Witteman, E.J.G. Sijbrands, A. Hofman, P.J. Koudstaal, M.M.B. Breteler, Insulin metabolism and the risk of Alzheimer disease: the Rotterdam study, *Neurology* 75 (2010) 1982–1987, <https://doi.org/10.1212/WNL.0b013e3181ffe4f6>.
- A.G. Vlassenko, T.L.S. Benzinger, J.C. Morris, PET amyloid-beta imaging in preclinical Alzheimer's disease, *Biochim. Biophys. Acta (BBA) - Mol. Basis Dis.* 1822 (2012) 370–379, <https://doi.org/10.1016/j.bbadis.2011.11.005>.
- O. Hansson, S. Lehmann, M. Otto, H. Zetterberg, P. Lewczuk, Advantages and disadvantages of the use of the CSF Amyloid β (A β) 42/40 ratio in the diagnosis of Alzheimer's disease, *Alzheimer's Res. Ther.* 11 (2019) 34, <https://doi.org/10.1186/s13195-019-0485-0>.
- E. Portelius, H. Zetterberg, U. Andreasson, G. Brinkmalm, N. Andreasen, A. Wallin, A. Westman-Brinkmalm, K. Blennow, An Alzheimer's disease-specific beta-amyloid fragment signature in cerebrospinal fluid, *Neurosci. Lett.* 409 (2006) 215–219, <https://doi.org/10.1016/j.neulet.2006.09.044>.
- N. Mizuta, K. Yanagida, T. Kodama, T. Tomonaga, M. Takami, H. Oyama, T. Kudo, M. Ikeda, M. Takeda, S. Tagami, M. Okochi, Identification of small peptides in human cerebrospinal fluid upon amyloid- β degradation, *Neurodegener. Dis.* 17 (2017) 103–109, <https://doi.org/10.1159/000453358>.
- W.B. Stine Jr., K.N. Dahlgren, G.A. Krafft, M.J. LaDu, In vitro characterization of conditions for amyloid-beta peptide oligomerization and fibrillogenesis, *J. Biol. Chem.* 278 (2003) 11612–11622, <https://doi.org/10.1074/jbc.M210207200>.
- T. Oe, B.L. Ackermann, K. Inoue, M.J. Borna, C.O. Garner, V. Gelfanova, R.A. Dean, E.R. Siemers, D.M. Holtzman, M.R. Farlow, I.A. Blair, Quantitative analysis of amyloid beta peptides in cerebrospinal fluid of Alzheimer's disease patients by immunoaffinity purification and stable isotope dilution liquid chromatography/negative electrospray ionization tandem mass spectrometry, *Rapid Commun. Mass Spectrom.* 20 (2006) 3723–3735, <https://doi.org/10.1002/rcm.2787>.
- M. Biancalana, S. Koide, Molecular mechanism of thioflavin-T binding to amyloid fibrils, *Biochim. Biophys. Acta Protein Proteomics* 1804 (2010) 1405–1412, <https://doi.org/10.1016/j.bbapap.2010.04.001>.
- S. Piovesana, C.M. Montone, C. Cavaliere, C. Crescenzi, G. La Barbera, A. Laganà, A.L. Capriotti, Sensitive untargeted identification of short hydrophilic peptides by high performance liquid chromatography on porous graphitic carbon coupled to high resolution mass spectrometry, *J. Chromatogr. A* 1590 (2019) 73–79, <https://doi.org/10.1016/j.chroma.2018.12.066>.
- Y.M. Kuo, T.A. Kokjohn, W. Kalback, D. Luehrs, D.R. Galasko, N. Chevallier, E. H. Koo, M.R. Emmerling, A.E. Roher, Amyloid- β peptides interact with plasma proteins and erythrocytes: implications for their quantitation in plasma, *Biochem. Biophys. Res. Commun.* 268 (2000) 750–756, <https://doi.org/10.1006/bbrc.2000.2222>.
- P.-P. Lin, W.-L. Chen, F. Yuan, L. Sheng, Y.-J. Wu, W.-W. Zhang, G.-Q. Li, H.-R. Xu, X.-N. Li, An UHPLC-MS/MS method for simultaneous quantification of human amyloid beta peptides A β 1-38, A β 1-40 and A β 1-42 in cerebrospinal fluid using micro-elution solid phase extraction, *J. Chromatogr. B* 1070 (2017) 82–91, <https://doi.org/10.1016/j.jchromb.2017.10.047>.
- S. Howell, J. Nalbantoglu, P. Crine, Neutral endopeptidase can hydrolyze β -amyloid(1-40) but shows no effect on β -amyloid precursor protein metabolism, *Peptides* 16 (1995) 647–652, [https://doi.org/10.1016/0196-9781\(95\)00021-b](https://doi.org/10.1016/0196-9781(95)00021-b).
- M.A. Leissring, A. Lu, M.M. Condron, D.B. Teplow, R.L. Stein, W. Farris, D. J. Selkoe, Kinetics of amyloid β -protein degradation determined by novel fluorescence- and fluorescence polarization-based assays, *J. Biol. Chem.* 278 (2003) 37314–37320, <https://doi.org/10.1074/jbc.M305627200>.
- Y. Shen, A. Joachimiak, M. Rich Rosner, W.-J. Tang, Structures of human insulin-degrading enzyme reveal a new substrate recognition mechanism, *Nature* 443 (2006) 870–874, <https://doi.org/10.1038/nature05143>.
- H. Im, M. Manolopoulou, E. Malito, Y. Shen, J. Zhao, M. Neant-Fery, C.-Y. Sun, S. C. Meredith, S.S. Sisodia, M.A. Leissring, W.-J. Tang, Structure of substrate-free human insulin-degrading enzyme (IDE) and biophysical analysis of ATP-induced conformational switch of IDE, *J. Biol. Chem.* 282 (2007) 25453–25463, <https://doi.org/10.1074/jbc.M701590200>.
- H. Kanemitsu, T. Tomiyama, H. Mori, Human neprilysin is capable of degrading amyloid β peptide not only in the monomeric form but also the pathological

- oligomeric form, *Neurosci. Lett.* 350 (2003) 113–116, [https://doi.org/10.1016/S0304-3940\(03\)00898-X](https://doi.org/10.1016/S0304-3940(03)00898-X).
- [37] K. Kidana, T. Tatebe, K. Ito, N. Hara, A. Kakita, T. Saito, S. Takatori, Y. Ouchi, T. Ikeuchi, M. Makino, T.C. Saido, M. Akishita, T. Iwatsubo, Y. Hori, T. Tomita, Loss of kallikrein-related peptidase 7 exacerbates amyloid pathology in Alzheimer's disease model mice, *EMBO Mol. Med.* 10 (2018), e8184, <https://doi.org/10.15252/emmm.201708184>.
- [38] Y. Hatakawa, R. Nakamura, M. Konishi, T. Sakane, A. Tanaka, A. Matsuda, M. Saito, T. Akizawa, Amyloid beta cleavage by ANA-TA9, a synthetic peptide from the ANA/BTG3 box A region, *Alzheimers Dement. (NY)* 7 (2021), e12146, <https://doi.org/10.1002/trc2.12146>.